Catalysis Today 141 (2009) 225–233

Contents lists available at ScienceDirect

Catalysis Today

journal homepage: www.elsevier.com/locate/cattod

Fe(III)-, Co(II)- and Ni(II)-impregnated MCM41 for wet oxidative destruction of 2,4-dichlorophenol in water

Suranjana Chaliha, Krishna G. Bhattacharyya *

Department of Chemistry, Gauhati University, Guwahati 781014, India

ARTICLE INFO

Article history:
Available online 23 May 2008

Keywords:
2,4-Dichlorophenol
Fe(III)-MCM41
Co(II)-MCM41
Ni(II)-MCM41
Wet oxidation

ABSTRACT

Chlorinated phenols, which enter water through effluents of petroleum and organochemical industry, are resistant to biological oxidation and are considered as problem pollutants. 2,4-Dichlorophenol (2,4-DCP), a member of the group, was chosen as the target compound in this study for destruction with wet oxidation using MCM41 impregnated with Fe(III)-, Co(II)- and Ni(II)-ions as the catalysts. The oxidation was carried out both in presence and in absence of H_2O_2 in a stirred reactor at 353 K under autogenous pressure of 0.2 MPa, catalyst load of $\geq$2 g/L and 2,4-DCP concentration of $\leq 10^{-3}$ M. 2,4-DCP destruction in a 1:1 molar mixture with H_2O_2 was 12.6, 19.7 and 35.4% with Fe(III)-, Ni(II)-, and Co(II)-MCM41, respectively, in 15 min of reaction time and was 38.6, 55.1 and 50.4% in 300 min. The oxidation was successful even without H_2O_2 when 18.9–45.7, 19.7–60.6 and 37.8–56.7% of 2,4-DCP was destroyed with Fe(III)-, Ni(II)- and Co(II)-MCM41, respectively, in 15–300 min. The effects of reaction time, catalyst load, 2,4-DCP concentration, reactant mole ratio, etc., were evaluated with suggestion of the possible mechanism. Fe(III)-, Co(II)- and Ni(II)-MCM41 have been shown to hold promise for wet catalytic destruction of 2,4-DCP.

1. Introduction

Phenolic compounds, which are generated by petroleum industries, coal conversion, and various organic chemical industries are common contaminants in wastewaters including those of pulp and paper mill effluent. In addition to these industries, olive oil production is another source for the release of phenol due to the high phenol content of olive mill effluents [1]. Phenols constitute one of the toxic groups of pollutants harmful to organisms and human health even at low concentrations [2]. Because of their toxicity, the US Environmental Protection Agency (EPA) has formulated regulatory measures for discharge of effluents containing chlorinated and other phenolic compounds [3–5]. Besides their toxic effects, phenolic compounds create an oxygen demand in receiving waters, and impart taste and odour to water even with trace concentrations of their chlorinated derivatives [1]. Taking all phenols together, US EPA has set a non-enforceable Human Health Water Quality standard of 2100 ppb [6].

Chlorophenols have found wide use in numerous applications and the wastewaters generated from such use contaminate the surrounding soil and water courses, affecting public health [7–12]. In particular, 2,4-dichlorophenol (2,4-DCP), a persistent pollutant frequently found in industrial effluents, is regarded as having relatively high toxicity. Although its use has been sought to be regulated because of its carcinogenic properties, still a large quantity of wastewater containing this pollutant continues to be discharged into the water environment [13]. 2,4-DCP is a chemical precursor that contributes principally to the manufacture of a widely used herbicide, 2,4-dichlorophenoxy acetic acid (2,4-D). After the herbicides have been applied to agricultural sites, 2,4-DCP remains as the major degradation product of conversion by photolysis and/or microbial activities in the soil or in water. 2,4-D is metabolized to 2,4-DCP by many fish species in water and the same type of metabolism takes place also in transgenic cotton plants. 2,4-DCP is also one of the products of water disinfection by chlorination and is a constituent of flue gas in municipal waste incineration and also of pulp and paper mill effluents [14]. Chlorophenols are normally resistant to biodegradation [15] and the preferred method of their removal has been either adsorption on activated carbon or oxidative destruction. Catalyst-based oxidation technologies using transition metal complexes have received considerable attention in recent years, but the main limitation is the difficult recovery of the complexes and their short lifetimes. Immobilization of transition metal complexes in different types of matrices and supports such as charcoal, polymers, zeolites and layered structures (pillared clays and hydrotalcites) either by direct intercalation, ion exchange or encapsulation has also been investigated [16]. Catalytic wet

---

* Corresponding author. Tel.: +91 361 2571529; fax: +91 361 2570599.
E-mail address: krishna2604@sify.com (K.G. Bhattacharyya).

0920-5861/$ – see front matter © 2008 Elsevier B.V. All rights reserved.
doi:10.1016/j.cattod.2008.03.011

oxidation of organic substances in wastewater considerably cuts down on energy and equipment costs compared to the non-catalytic process, which requires very high temperature and pressure [17]. The catalyst is normally dispersed in the reaction medium in the form of metal ions, or fine particles of oxides providing maximum specific surface area. The fine particles being unstable often aggregate into bigger ones resulting in a rapid loss of surface area and hence, the catalytic activity. This problem is usually overcome by dispersing the catalyst components on a porous support.

The choice of a catalyst support largely depends on the surface area and pore size of the support itself. High surface area could provide high population of the active sites while large pore size allows the accessibility of the reactants to approach those catalytic active sites. The regular, hexagonal mesoporous structure of MCM41 (with uniform pore openings of 15–100 Å) and the potential modification of its properties by introduction of specific transition metal cations or metal complexes have made MCM41 an interesting material in this regard [18]. The pore size control in MCM41 could be achieved by a suitable choice of template or by changing synthesis conditions.

Attempts to insert transition metals, such as Cu [17], Ti, Cr, Mn or Fe into the MCM41 framework have been reported recently [18]. The oxidizing ability of MCM41 synthesized hydrothermally and substituted with transition metal ions, either isomorphously or by impregnation has received considerable attention. Wu et al. [17] used Cu-MCM41 for oxidation of phenol in aqueous medium. Wet oxidation of anthracene and *trans*-stilbene over modified MCM41 has also been reported [18].

This study incorporates preparation and characterization of MCM41 impregnated with Fe(III), Co(II) and Ni(II) and utilization of the mesoporous materials for wet oxidation of 2,4-dichlorophenol in water with and without the presence of the common oxidizing agent, H_2O_2.

2. Experimental

2.1. Chemicals used

Commercially available aluminum sulphate (E. Merck, Mumbai, India), sodium hydroxide (E. Merck, Mumbai, India), tetramethylammonium hydroxide pentahydrate (Fluka, Steinheim, Switzerland), silica fumed (Sigma, St. Louis, MO, USA), hexadecyltrimethylammonium chloride (Fluka, Steinheim, Switzerland) were used for synthesizing the support, MCM41. Iron(III) nitrate nonahydrate, cobalt(II) nitrate hexahydrate and nickel(II) nitrate (all, E. Merck, Mumbai, India) were used for metal incorporation. 2,4-Dichlorophenol (minimum assay >98%) for the reactions was procured from Merck-Schuchardt, Honenbrunn, Germany. All other chemicals used were of analytical grade.

2.2. Synthesis of Fe(III)-, Co(II)- and Ni(II)-impregnated MCM41

MCM41 was synthesized [19] by mixing together aqueous solutions of aluminium sulphate (0.62 g) and sodium hydroxide (0.3 g) dissolved in minimum volume of water in a 250 mL Teflon-lined beaker and stirring the same continuously till a clear solution was obtained. Tetramethyl ammonium hydroxide (9.4 g) and fumed silica (9.26 g) were then added under stirring condition at room temperature. Hexadecyltrimethylammonium chloride (10.55 g) was added slowly and the pH of the mixture was maintained at 11.0 by adding sodium hydroxide pellets if necessary. Stirring was continued till a fine gel was obtained. The composition of the gel was 1.0 SiO_2:0.27 HDTMACl:0.06 $Al_2(SO_4)_3\cdot18H_2O$:0.03 Na_2O:0.33 TMAOH:20 H_2O. The gel was transferred into an autoclave and was kept at 373 K for 24 h. The crystals of MCM41 were recovered by filtration, washed with deionized water, dried in air and calcined at ~823 K in air for 5 h. Fe(III)-, Co(II)- and Ni(II)-impregnated MCM41 was prepared by mixing together equal amounts of MCM41 and iron(III) nitrate or cobalt(II) nitrate or nickel(II) nitrate, using minimum volume of water for wetting, followed by evaporation of the solvent at 393 K for 5 h and calcination at 773–873 K for 5 h in air.

2.3. Catalyst characterization

Metal supported MCM41 synthesis was confirmed by XRD measurements (Philips Analytical X-Ray Spectrophotometer, PW 1710, Cu Kα radiation, Almelo, The Netherlands). The changes in surface topography following metal impregnation were observed with SEM (LEO-1430 VP, Carl Zeiss, UK). The percentage of Fe(III), Co(II) and Ni(II) entering into MCM41 is determined with Atomic Absorption Spectrophotometer (Varian SpectrAA220, Australia). The catalysts were further characterized by FTIR measurements (PerkinElmer Spectrum RXI, range 4400–440 cm^{-1}, MA, USA) using KBr self-supported pellet technique. The cation exchange capacity (CEC) of the catalysts was estimated using the copper bisethylenediamine complex method [20].

2.4. Wet oxidation of 2,4-DCP

Catalytic oxidation was carried out in a high-pressure stirred reactor (Toshniwal Instruments, Nashik, India) under the following conditions:

Feed volume	25 mL 2,4-DCP, 25 mL H_2O_2 (in absence of H_2O_2, 2,4-DCP 50 mL)
Concentration	2,4-DCP 10^{-3} M (except when monitoring effects of concentration)
H_2O_2 concentration	10^{-3} M or as stated
Catalyst load	0.1 g/50 mL (2 g/L) or as stated
Temperature	353 K
Pressure	0.2 MPa (autogeneous)
Stirrer speed	180 rpm
Time	5 h or as stated

After the reaction was over, the mixture was centrifuged and the unconverted reactant was estimated in the supernatant layer spectrophotometrically (Hitachi U3210).

Product identification was done with GC–MS (Shimadzu GC 2010, Columbia, USA) using Rtx 5 column of length 30 m, diameter 0.25 mm and film (poly(5% diphenyl 95% dimethyl)silanone) thickness 0.25 μm under temperature programmed mode from 40 to 240 °C (36 min). 0.6 μL of the product mixture was injected into the GC–MS in each run.

3. Results and discussion

3.1. Catalyst characterization

3.1.1. XRD study

The uncalcined MCM41 showed only one prominent diffraction peak at $2\theta = 2.57^\circ$ ($d = 34.33$ Å) followed by a broad band, while the calcined form showed three peaks at $2\theta = 2.37^\circ$ ($d = 37.32$ Å), 4.1° ($d = 21.81$ Å) and 4.74° ($d = 18.63$ Å). These results are in conformity with the literature values for MCM41 [17], known to give three to five reflections between 2° and 5° indicating long range order in them, although samples with more reflections have also

Table 1
XRD characteristics of uncalcined (A), calcined (B) and Fe(III)-, Co(II)- and Ni(II)-incorporated MCM41

Catalysts	Angle (2θ°)	d-spacing (Å)	a_o (Å)
MCM41(A)	2.57	34.3	39.6
MCM41(B)	2.37	37.3	43.1
	4.10	21.8	
	4.74	18.6	
Fe(III)-MCM41	3.39	26.1	30.1
	3.92	22.5	
Co(II)-MCM41	3.96	22.3	25.8
Ni(II)-MCM41	2.99	29.5	34.0
	4.04	21.8	

been reported. These reflections are assigned to the ordered hexagonal array of parallel silica tubes and can be indexed as (1 0 0), (1 1 0), (2 0 0), (2 1 0) and (3 0 0) reflections assuming a hexagonal unit cell. In the present study, the calcined MCM41 yielded three XRD peaks in the said region and the most prominent peak at $2\theta = 2.37°$ could be attributed to (1 0 0) reflection. The MCM41 materials are not crystalline at the atomic level, and therefore, no reflections at higher angles are expected. The reflections at higher angles would any way be very weak because the structural features have very little influence at higher angles. In the metal-impregnated MCM41 materials, the prominent (1 0 0) reflection ($2\theta = 2.37°$) was either masked or shifted. Thus, calcined samples of MCM41 impregnated with Fe(III), Co(II), and Ni(II) showed the following prominent peaks:

(a) Fe(III)-MCM41: 3.39° ($d = 26.05$ Å) and 3.92° ($d = 22.49$ Å),
(b) Co(II)-MCM41: 3.96° ($d = 22.31$ Å) and
(c) Ni(II)-MCM41: 2.99° ($d = 29.46$ Å) and 4.04° ($d = 21.84$ Å).

The XRD characteristics including the hexagonal unit cell length (a_o) are given in Table 1. The shift in (1 0 0) reflection band and changes in the other characteristics due to metal-impregnation show that the structural regularity of the materials is affected to different extents as is also observed by other workers [18]. The incorporation of metal ions has led to distortion of the hexagonal regularity manifesting itself in peak broadening and the observed shift. When the XRD characteristics of the calcined MCM41 and the calcined samples of impregnated MCM41 are compared, it is seen that the highest distortion in the regular structure was caused by incorporation of Co(II) followed by Fe(III) and Ni(II). With respect to (1 0 0) reflection band, the changes in d-spacing are in conformity with the above order, i.e. Co(II) > Fe(III) > Ni(II). The incorporation of Co(II) into MCM41 brought about the largest decrease in the hexagonal unit cell length followed by Fe(III) and Ni(II).

3.1.2. Scanning electron microscopy study

Scanning electron micrographs of calcined samples of MCM41, Fe(III)-MCM41, Co(II)-MCM41 and Ni(II)-MCM41 are shown in Fig. 1(a) and (b). Introduction of Fe(III), Co(II) and Ni(II) into MCM41 influenced the morphology of the mesoporous material. The grains of the salts could be clearly seen distributed over the MCM41 particles. No significant difference could be observed between Fe(III)-MCM41 and Co(II)-MCM41 with respect to morphology, but Ni(II)-MCM41 showed a slightly different morphology with the salt grains having some preferential distribution.

3.1.3. FTIR study

FTIR spectra of calcined samples of Fe(III)-, Co(II)- and Ni(II)-MCM41 showed the same prominent bands as found in the calcined MCM41 (Fig. 2). For example, uncalcined MCM41, calcined MCM41, Fe(III)-MCM41, Co(II)-MCM41, and Ni(II)-MCM41 showed IR bands at 960, 965, 967, 966, and 964 cm^{-1}. The band around 960 cm^{-1} is normally assigned to lattice defect

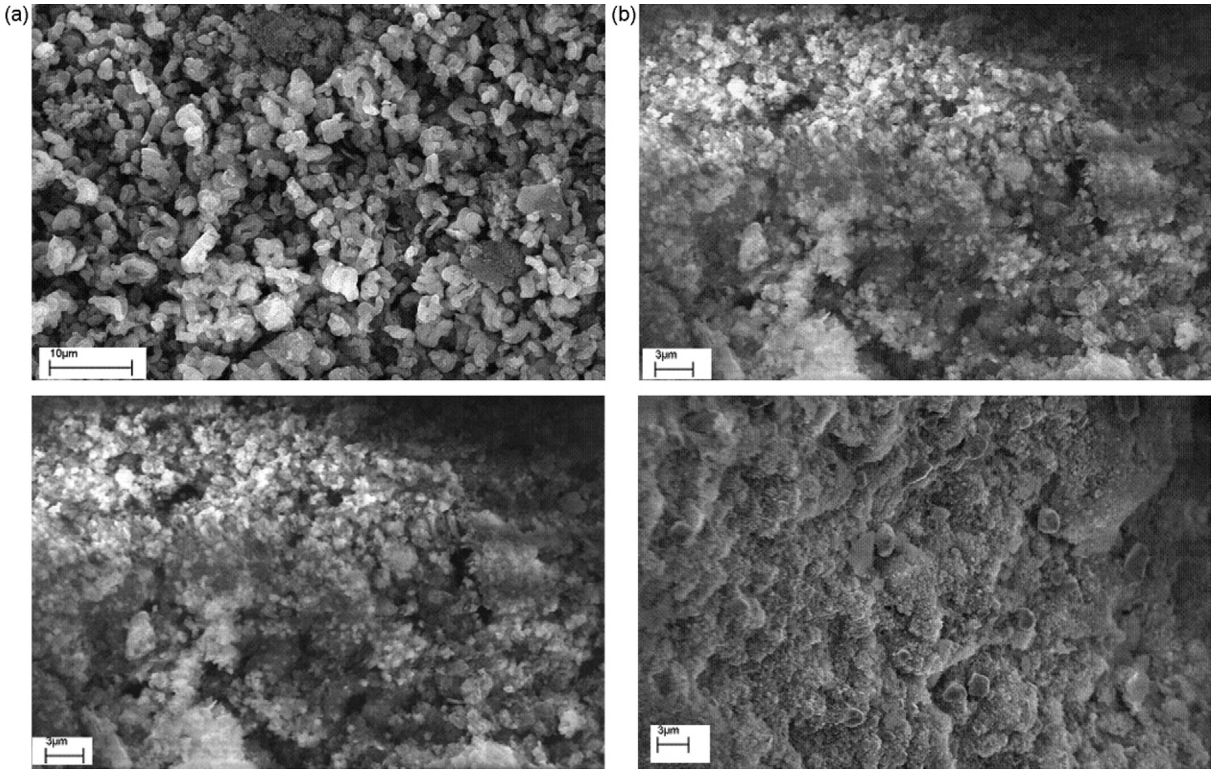

Fig. 1. (a) SEM photographs of calcined MCM41 (top) and Fe(III)-MCM41 (bottom), (b) SEM photographs of Co(II)-MCM41 (top) and Ni(II)-MCM41 (bottom).

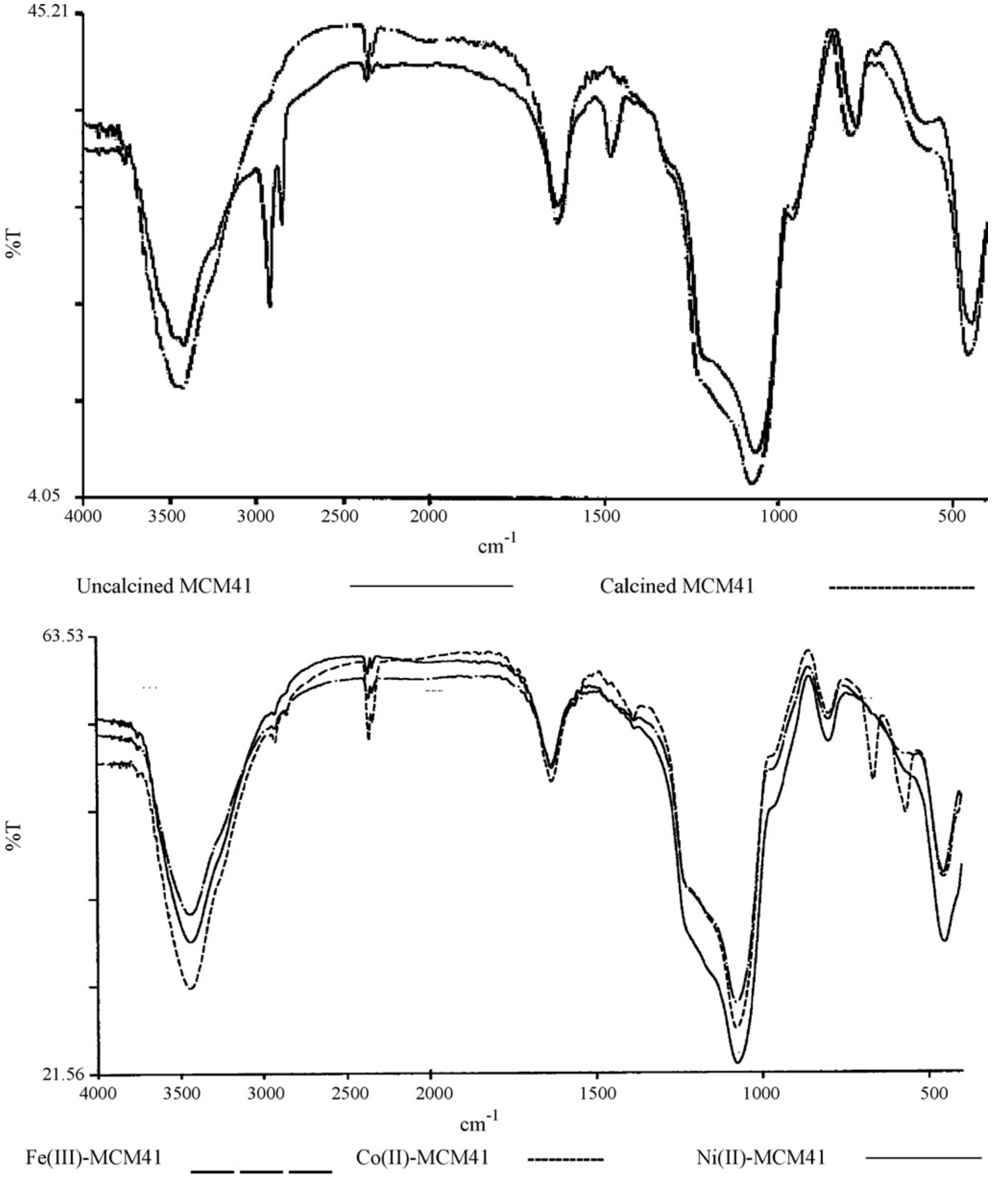

Fig. 2. FT-IR spectra of uncalcined and calcined MCM41 (top) and of calcined samples of Fe(III), Co(II) and Ni(II) supported on MCM41 (bottom).

and is correlated with the presence of tetrahedral framework linkages of the type M–O–Si [21,18]. This band has been known to undergo slight red shift on metal-incorporation. Such shift was visible in all the cases in the present study. Assignment of this band to a Si–O vibration in Si–OH groups in siliceous MCM41 has also been suggested [22]. If this is the case, it is reasonable to attribute the red shift in metal incorporated MCM41 to the replacement of H from an OH group by a metal ion to form O–M type linkage.

The broad absorption band between 3650 and 3400 cm^{-1} in the FTIR spectra (3430 cm^{-1} in uncalcined MCM41, 3434 cm^{-1} in calcined MCM41, 3447 cm^{-1} in Fe(III)-MCM41, 3450 cm^{-1} in Co(II)-MCM41 and 3460 cm^{-1} in Ni(II)-MCM41) may be attributed to hydrogen-bonded vicinal pairs of silanol groups [23]. The broad band between 1000 and 1250 cm^{-1} in the MCM41 samples (1100 and 1210.3 cm^{-1} in uncalcined MCM41, 1090 and 1206 cm^{-1} in calcined MCM41, 1090 and 1199 cm^{-1} in Fe(III)-MCM41, 1089 and 1219 cm^{-1} in Co(II)-MCM41, 1083 and 1219 cm^{-1} in Ni(II)-MCM41) may be assigned to the asymmetric stretching of Si–O–Si bridges. IR bands in the regions, 720–740 cm^{-1} and 1400–1500 cm^{-1} have been shown to correspond to aliphatic C–H bending vibrations and in the region, 2800–3100 cm^{-1} to aliphatic C–H stretching vibration [24]. In the present work, no significant band was observed in the region of aliphatic C–H bending, but a few bands could be seen for aliphatic C–H stretching (2923 cm^{-1} uncalcined MCM41, 2930 cm^{-1} Fe(III)-MCM41, 2920 cm^{-1} Co(II)-MCM41 and 2925 cm^{-1} Ni(II)-MCM41). Some other bands observed in the present work (799 cm^{-1} uncalcined MCM41, 794 cm^{-1} calcined MCM41, 797 cm^{-1} Co(II)-MCM41, 799 cm^{-1} Ni(II)-MCM41 and 802 cm^{-1} Fe(III)-MCM41) could not be properly assigned. The C–H stretching and bending vibrations obviously refer to the presence of the template or its fragments in the material synthesized which might indicate that calcination did not completely remove the template used in synthesis of MCM41.

3.1.4. AAS measurement

AAS measurement of the metal-impregnated MCM41 materials showed that 0.36, 1.91, and 2.20% (by weight) of Fe(III), Co(II) and Ni(II), respectively, had entered into the mesoporous material. The impregnation was done by treating 0.1 g of MCM41 with 0.1 g of a water soluble salt of the metal (containing 0.014 g Fe(III), 0.020 g

Co(II) and 0.020 g Ni(II) in 0.1 g of salt). The actual amount of metal that entered into MCM41 was Fe(III): 3.55 mg/g, Co(II): 19.08 mg/g and Ni: 22.03 mg/g.

3.1.5. Cation exchange capacity (CEC)

The CEC of MCM41 was measured as 0.205 meq/g. There is significant change on metal incorporation into MCM41 by the impregnation technique as the CEC of Fe(III)-, Co(II)- and Ni(II)-supported MCM41 increased to 0.255, 0.242 and 0.260 meq/g. The CECs of the three metal-impregnated MCM41 differed from one another by an appreciable amount, and the difference was quite significant when compared to the CEC of the parent MCM41. The ion exchange capacity may be attributed to structural defects, broken bonds and structural hydroxyl transfers as in the case of clays [25], and the values indicate that introduction of Fe(III)-, Co(II) and Ni(II) enhanced the same by 24.4, 18.0, 26.8%, respectively. Thus, incorporation of Fe(III), Co(II) and Ni(II) into MCM41 has resulted in a substantial increase in the number of exchange sites which followed the order Ni(II) > Fe(III) > Co(II). However, since the AAS measurements have indicated the actual amount of the metal ions entering into MCM41 to be in the order of Ni(II) > Co(II) > Fe(III), it is likely that the trivalent Fe ions have a much greater influence on promoting cation exchange.

3.2. Wet oxidation of 2,4-dichlorophenol

The activities of Fe(III)-MCM41, Co(II)-MCM41 and Ni(II)-MCM41 as environment-friendly catalysts are determined with respect to wet oxidation of 2,4-dichlorophenol.

3.2.1. Effects of reaction time and kinetics

Reaction time (15–300 min) had similar effects on catalytic wet oxidation of 2,4-dichlorophenol (Fig. 3). Conversion increases with time till equilibrium conditions are approached. Some differences exist between the situations when hydrogen peroxide is present and when the reactions are carried out without it. The conversion of 2,4-DCP in presence of H_2O_2 after 15 min of reaction was 12.6, 19.7 and 35.4%, respectively, for Fe(III)-, Ni(II)-, and Co(II)-MCM41, which increased to 38.6, 55.1 and 50.4% after 300 min. The catalyst load was uniform in all the cases (2 g/L) although the metal loadings were not the same.

Fig. 3 shows that 2,4-DCP breaks down even without any H_2O_2 in the reaction mixture when it is stirred in presence of the catalyst. Under such circumstances, the catalyst Fe(III)-MCM41 gave 18.9–45.7% conversion in the time interval of 15–300 min. The conversions brought about by Ni(II)-MCM41 and Co(II)-MCM41 in the same time interval were 19.7–60.6 and 37.8–56.7%, respectively. It is to be noted that the conversions without hydrogen peroxide were either lower than or similar to those with hydrogen peroxide when the reaction time was not very large, but with increasing reaction time, the conversion without hydrogen peroxide became better in case of all the catalysts.

Srinivas et al. [18] have prepared oxidation catalysts by incorporating a number of transition metals (Ti, V, Cr, Mn, Fe, Co, Ni, Cu, Zn) into MCM41 by impregnation. On testing the effectiveness of the catalysts for oxidation of anthracene by measuring the selectivity of one of the oxidation products, 9,10-anthraquinone, it was found by the authors that the catalysts can be arranged in the order of Cr-MCM41 > Mn-MCM41 > Co-MCM41 > Cu-MCM41 > Fe-MCM41 > V-MCM41 > Ni-MCM41 > Zn-MCM41 > Ti-MCM41. However, the conversion takes place very slowly and a maximum of 70% conversion could be achieved over a longer oxidation period of 20 h or more. In the present study, the total conversion followed the order: Ni(II)-MCM41 > Co(II)-MCM41 > Fe(III)-MCM41. The conversion was fast and a conver-

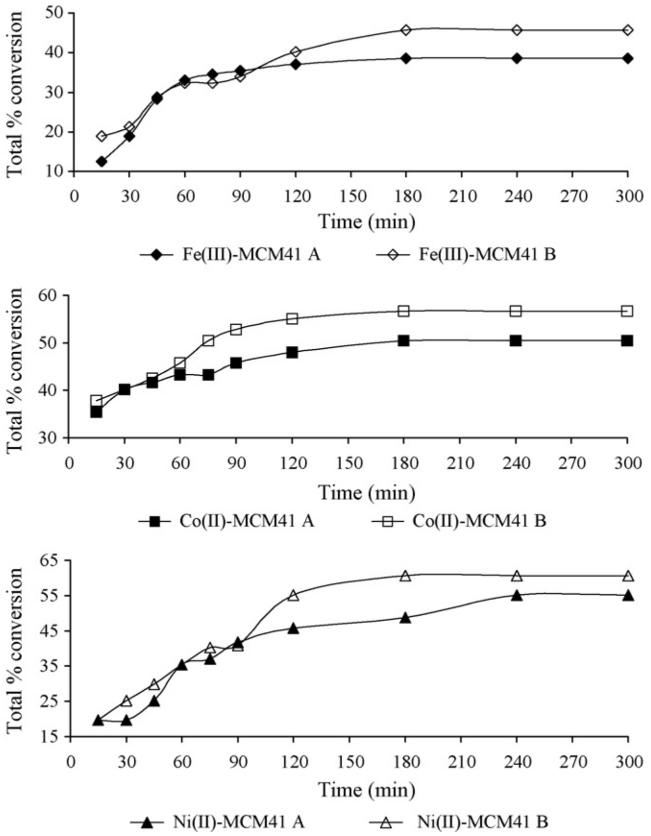

Fig. 3. Effect of reaction time on wet oxidation of 2,4-DCP (1×10^{-3} M) ((A) 2,4-DCP:H_2O_2 mole ratio 1:1, (B) without H_2O_2, temperature 353 K, catalyst load 2 g/L).

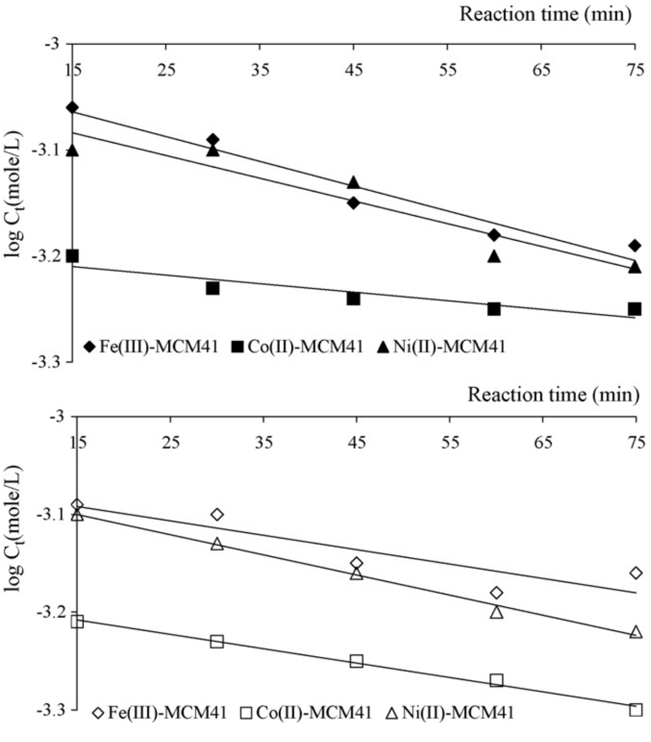

Fig. 4. The first-order degradation of 2,4-DCP (1×10^{-3} M) by wet oxidation at 353 K (catalyst load 2 g/L; top 2,4-DCP:H_2O_2 mole ratio 1:1; bottom without H_2O_2).

Table 2
Apparent kinetic constant (k) and the regression coefficient (R) for the degradation of 2,4-DCP on wet oxidation (2,4-DCP 1×10^{-3} M; temperature 353 K; catalyst load 2 g/L; (A) 2,4-DCP:H_2O_2 mole ratio 1:1; (B) without H_2O_2)

Catalyst	A		B	
	k (L (g catal)$^{-1}$ min^{-1})	R	k (L (g catal)$^{-1}$ min^{-1})	R
Fe(III)-MCM41	5.3×10^{-3}	0.97	4.4×10^{-3}	0.9
Co(II)-MCM41	5.0×10^{-3}	0.94	3.5×10^{-3}	1.0
Ni(II)-MCM41	4.8×10^{-3}	0.94	4.8×10^{-3}	1.0

sion of about 60% could be obtained in a shorter reaction time of 3 h.

Application of the first-order kinetics to the catalytic wet oxidation of 2,4-dichlorophenol over Fe(III)-, Co(II)- and Ni(II)-MCM41 according to the equation:

$$C_t = C_o \, e^{-kt}$$

or,

$$\log C_t = \log C_o - \left(\frac{k}{2.303}\right)t$$

yielded linear log C_t vs. time curves (Fig. 4) up to a reaction time of 75 min. Therefore, at least in the initial stages of the reaction, 2,4-DCP oxidation follows first-order kinetics and the conversion is independent of 2,4-DCP concentration. The values of the linear regression coefficient and the apparent kinetic constant obtained from Fig. 4 are presented in Table 2. The apparent kinetic constants show small differences with respect to the presence or absence of H_2O_2—the values being 5.3×10^{-3}, 5.0×10^{-3} and 4.8×10^{-3} L (g catal)$^{-1}$ min^{-1} with H_2O_2 and 4.4×10^{-3}, 3.5×10^{-3} and 4.8×10^{-3} L (g catal)$^{-1}$ min^{-1} without H_2O_2 for Fe(III)-, Co(II)- and Ni(II)-MCM41, respectively.

Very few works have been reported on kinetics of catalytic oxidation of 2,4-DCP and similar compounds. Oliveira et al. [12] have shown that oxidation with Fenton's reagent is an efficient and fast process for 2,4-DCP degradation. The pseudo-first-order model has been shown to hold good at least for the initial stage of the reaction when several competitive reactions are likely to consume the hydroxyl radicals forming a number of intermediate products from 2,4-DCP decomposition. The decomposition apparently involved several reactions with iron(II) and iron(III) species, hydrogen peroxide, hydroxyl radicals, and the organic substrate [11]. All of these point to a complicated kinetic mechanism of 2,4-DCP degradation.

3.2.2. *Effects of mole ratio of the reactants*

The influence of the mole ratio of the reactant feed (H_2O_2 to 2,4-DCP) was studied for mole ratios of 1:1 to 20:1 while keeping the reaction time (300 min) and catalyst load (2 g/L) constant. The results showed a considerable influence of the mole ratio on the overall conversion (Fig. 5). Increasing the relative amount of H_2O_2 in the reaction mixture destroyed more and more 2,4-DCP with Co(II)-MCM41 as the most effective catalyst in presence of the oxidizing agent H_2O_2. Fe(III)-, Co(II)- and Ni(II)-MCM41 gave total 2,4-DCP conversion of 38.6–50.5, 50.4–55.5 and 55.1–65.1%, respectively, with the mole ratio (H_2O_2 to 2,4-DCP) of 1:1 to 20:1.

The stoichiometric equation for the complete oxidation of 2,4-DCP with H_2O_2 as given below indicates that the mole ratios of 1:12 would be most suitable for bringing about complete oxidation of 2,4-DCP

$$2,4\text{-DCP}: \quad C_6H_3Cl_2(OH) + 12H_2O_2 \rightarrow 6CO_2 + 13H_2O + 2HCl$$

In oxidation of anthracene to *tert*-butylhydroperoxide (*t*-BHP), Srinivas et al. [18] observed an increase in conversion up to >90% when the mole ratio of anthracene to *t*-BHP was increased from 1:2 to 1:10. Although stoichiometrically 1:2 ratio of oxidant was sufficient to bring about the oxidation, the requirement of much higher mole ratio with respect to *t*-BHP is attributed to non-selective thermal decomposition of the peroxide.

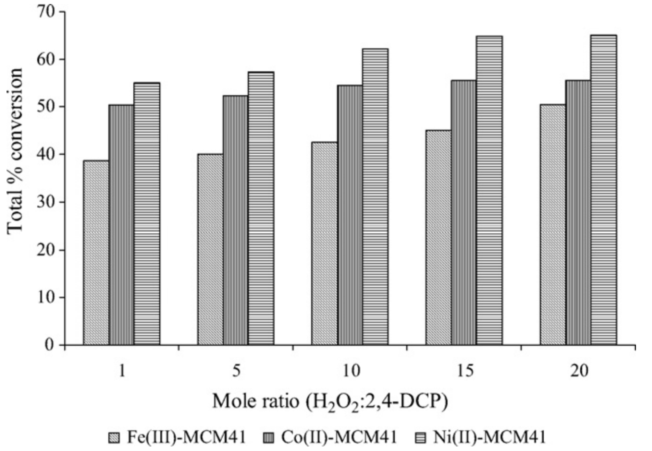

Fig. 5. Effects of mole ratio of feed (H_2O_2:2,4-DCP) on wet oxidation of 2,4-DCP (10^{-3} M) with H_2O_2 at 353 K (reaction time 300 min, catalyst load 2 g/L).

3.2.3. *Effects of catalyst load*

When the catalyst load was increased from 2–10 g/L in five steps keeping the reaction time constant (300 min) with or without H_2O_2 in the reaction mixture, the total conversion of 2,4-DCP (Table 3) showed reasonable enhancement. At the lowest catalyst load of 2 g/L, Ni(II)-MCM41 could convert 55.1% of 2,4-DCP in presence of H_2O_2 compared to 38.6% for Fe(III)-MCM41 and 50.4% for Co(II)-MCM41. The conversion at the highest catalyst load of 10 g/L was Fe(III)-MCM41: 50.0%, Co(II)-MCM41: 60.8% and Ni(II)-MCM41: 68.0%. When the reaction was carried out under the same set of conditions as above but without taking the oxidant H_2O_2 in the reactant feed, the conversion at the highest catalyst load of 10 g/L followed the order Ni(II)-MCM41 (66.4%) > Co(II)-MCM41 (60.0%) > Fe(III)-MCM41 (48.8%) (Table 3). These results show that almost the same level of conversion of 2,4-DCP was maintained with Co(II)-MCM41 whether H_2O_2 was present or not, but better conversion was possible with Ni(II)-MCM41 and Fe(III)-MCM41 if H_2O_2 was present.

As free metals, Fe chemisorbs oxygen much more strongly than Co and Ni, the latter two having similar chemisorption abilities [26] and their catalytic properties could be understood on the basis of their electronic structure, particularly of the surface atoms. The situation becomes much more complicated when instead of free metal atoms, ions have to be considered. Since Fe chemisorbs oxygen molecules very strongly, it is likely that the Fe(III) ions release fewer oxygen atoms to undergo reaction with 2,4-DCP and

Table 3
Effects of catalyst load on wet oxidation of 2,4-DCP at 353 K (reaction time 300 min, 2,4-DCP 1×10^{-3} M, (A) 2,4-DCP:H_2O_2 mole ratio 1:1, (B) without H_2O_2)

Catalyst (g/L)	Total conversion (%) of 2,4-DCP					
	Fe(III)-MCM41		Co(II)-MCM41		Ni(II)-MCM41	
	A	B	A	B	A	B
2	38.6	45.7	50.4	56.7	55.1	60.6
4	41.0	47.1	60.8	57.1	56.4	62.3
6	47.1	48.0	60.8	58.2	65.0	65.0
8	50.0	48.8	60.8	60.0	68.0	66.4
10	50.0	48.8	60.8	60.0	68.0	66.4

Table 4
Effects of concentration of 2,4-DCP on its wet oxidation at 353 K (reaction time 300 min, catalyst load 2 g/L, (A) H_2O_2 2×10^{-4} M, (B) without H_2O_2)

2,4-DCP concentration (M)	Total conversion (%) of 2,4-DCP					
	Fe(III)-MCM41		Co(II)-MCM41		Ni(II)-MCM41	
	A	B	A	B	A	B
2×10^{-4}	70.0	70.5	62.7	65.0	70.8	68.0
4×10^{-4}	54.5	65.5	60.6	62.5	68.3	66.3
6×10^{-4}	53.1	58.9	60.1	60.0	65.8	64.8
8×10^{-4}	45.5	52.3	58.7	58.4	63.3	62.5
10×10^{-4}	38.6	45.7	50.4	56.7	55.1	60.6
% Decrease	44.9	35.2	19.6	12.8	22.2	10.9

consequently, Fe(III)-MCM41 showed the least conversion of 2,4-DCP. The differences between the catalytic activities of Co(II)-MCM41 and Ni(II)-MCM41 might be due to the intricate differences in their electronic structures [d^7 for Co(II) and d^8 for Ni(II)], particularly the number of unpaired d-electrons which are responsible for binding the chemisorbed oxygen molecules to the catalyst surface in a precursor state before chemisorption occurs. Co(II) and Ni(II) are therefore expected to behave differently when chemisorbing oxygen directly from the atmosphere or O-atom (or OH radicals) from the decomposition of H_2O_2.

3.2.4. Effects of 2,4-DCP concentration

If the concentration of 2,4-DCP was increased, the conversion after a fixed reaction time of 300 min showed a downward trend (Table 4). With the concentration of 2,4-DCP increasing from 2×10^{-4} to 10×10^{-4} M with a constant concentration of H_2O_2 (2×10^{-4} M), the conversion came down from 70.0–38.6% for Fe(III)-MCM41, 62.7–50.4% for Co(II)-MCM41, and 70.8–55.1% for Ni(II)-MCM41. The pattern was similar when no H_2O_2 was present and the conversion decreased from 70.5–45.7% for Fe(III)-MCM41, 65.0–56.7% for Co(II)-MCM41, and 68.0–60.6% for Ni(II)-MCM41. The conversion is now fully dependent on 2,4-DCP concentration the effect being most significant with respect to the activity of Fe(III)-MCM41 catalyst, which shows a decrease in the total conversion by 44.9 and 35.2% with and without H_2O_2. For Co(II)-MCM41 and Ni(II)-MCM41, the decrease in total conversion was between 10 and 23% only in the same concentration range of 2,4-DCP.

Thus, although a first-order kinetic mechanism has been shown to be working satisfactorily in the initial stages of the reaction with 2,4-DCP concentration of 10^{-3} M, the same does not hold good with increase in reaction time as well as 2,4-DCP concentration. Under such conditions, the reaction mechanism is not likely to be governed by the simple processes of adsorption on the catalyst surface, interaction with OH radicals, formation of degradation products and their desorption from the solid surface, but the processes are now likely to be controlled by a transport mechanism involving diffusion of 2,4-DCP molecules from the aqueous phase to the surface of the catalyst as well as diffusion of the degradation products from the solid surface back to the aqueous phase.

3.2.5. Mechanism of oxidative destruction

A mechanism for 2,4-DCP oxidation is suggested based on (i) known products of degradation of 2,4-DCP, and (ii) products identified in the reactions. GC–MS analysis of the products was able to identify several likely oxidation products such as (i) chlorocatechol, (ii) 2-chloro-1,4-benzoquinone, (iii) maleic acid, (iv) fumaric acid, (v) acrylic acid and (vi) malonic acid.

The proposed mechanism is based on OH radicals acting as the destroyer, as in the case of common oxidation reactions where hydrogen peroxide is the oxidizing agent. The OH radicals in the present case are likely to have their origin in the metal oxides formed during calcination of the catalysts. Formation of OH-radicals on the surface of the catalysts will follow from interactions between excited O-atoms of the catalyst and H-atoms cleaved from the substrate or even water since the reactions were carried out in aqueous solution [27]. Participation of dissolved oxygen in OH-radical formation is not likely since this will result in a drastic reduction in oxidation with increase in reaction temperature (consequent decrease in dissolved oxygen level).

The hydroxyl radicals attack 2,4-DCP at the positions of the two Cl-atoms (Scheme 1). In the process, the OH groups successively replace the electron-withdrawing Cl-atoms converting 2,4-DCP (I) first to chlorocatechol (II, III), then to chlorobenzoquinone (IV) and finally to unsaturated dicarboxylic acids (V). OH groups also interact with the unsaturated dicarboxylic acids transforming them into simple acids like acetic acid, oxalic acid, etc., as the final products.

It is proposed that the chlorinated hydroquinone (III) after the first step leaves off two hydrogen atoms to give the corresponding

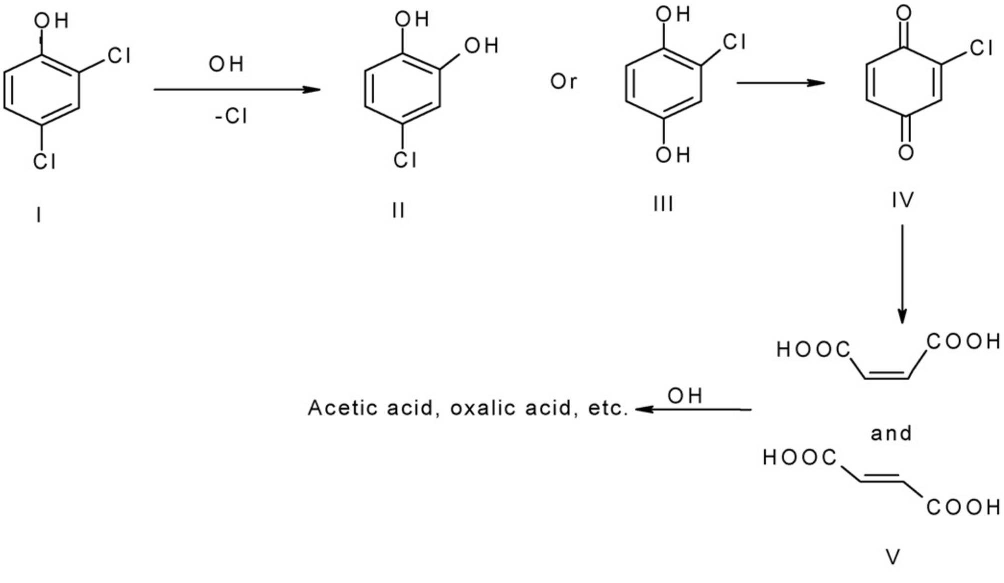

Scheme 1.

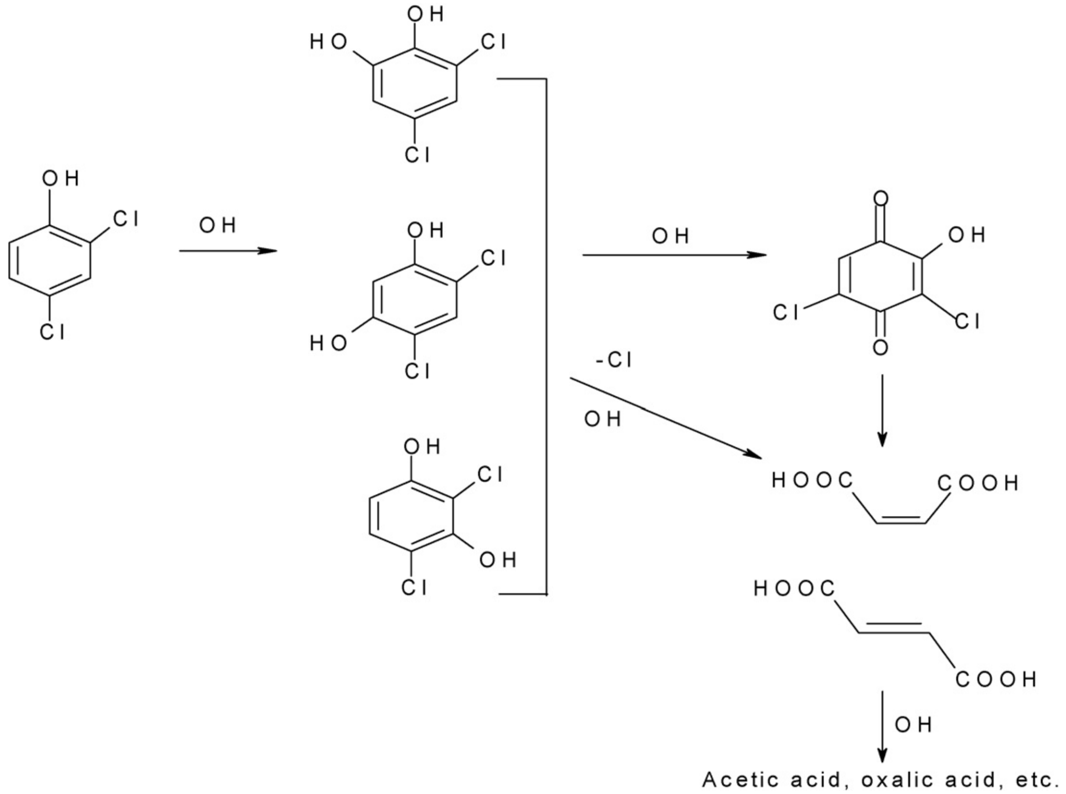

Scheme 2.

quinone, such as 2-chloro-1,4-benzoquinone (IV), in response to further hydroxyl radical attacks. 2-Chloro-1,4-benzoquinone is likely to be the dominant quinone because the *para*-site is usually the preferred location for HO attacks on 2,4-DCP and the Cl-atom at the *ortho*-site is somewhat protected from further attack due to steric effect of the nearby hydroxyl group, while such hindrance is not there for the *para*-site. A similar observation was also reported in the photodegradation of 2,4-dichlorophenoxyacetic acid over titanium dioxide suspensions [14].

The mechanism may also follow another route as shown in Scheme 2. In this route, an electrophilic OH group is added onto the aromatic ring of the 2,4-DCP, leading to the formation of isomers 3,5-dichlorocatechol, 2,4-dichlororesorcinol and 4,6-dichlororesorcinol. The three isomers undergo further hydroxylation and the intermediates thus produced rapidly dehydrogenate to their corresponding quinones, one of which has been identified as 3,5-dichloro-2-hydroxy-1,4-benzoquinone. The benzoquinones are converted to the simple organic acids by the same route as in Scheme 1.

It has already been reported that hydroxyl radicals could break aromatic rings of chlorobenzo-quinone and other hydroxylated products, resulting in formation of maleic acids, fumaric acids, and simpler organic acids (via decarboxylation) including acetic acid, formic acid, glyoxylic acid, and oxalic acid [14]. If there are no additional radical competitors in the solution, these low molecular organic acids can gradually be mineralized to carbon dioxide.

Whatever mechanism is followed, it is clear that much more work is necessary to find out the slowest or the rate-determining step, and therefore to suggest the exact kinetic mechanism by which 2,4-DCP oxidation proceeds.

4. Conclusion

Incorporation of Fe(III), Co(II) and Ni(II) into MCM41 has produced supported metal catalysts with reasonable activity towards oxidative destruction of 2,4-DCP. That the catalysts can bring about wet air oxidation without an oxidant like H_2O_2 is an additional advantage and will certainly cut down on costs involved. The degradation of 2,4-DCP takes place very rapidly following a first-order reaction kinetics initially and the destruction of the pollutant in effluents should not take a long time.

References

[1] S. Yapar, M. Yilmaz, Adsorption 10 (2004) 287.
[2] W. Bruce, M.E. Meek, A. Newhook, Environ. Carcinogen. Ecotoxicol. Rev. C19 (2001) 305.
[3] US EPA, Federal Register, vol. 52, Washington, DC, USA, 1987, p. 25861.
[4] P. Bajpai, P.K. Bajpai, J. Biotechnol. 33 (1994) 211.
[5] I. Rodriguez, M.P. Llompart, R. Cela, J. Chromatogr. 885 (2000) 291.
[6] EPA, Drinking water standards and health advisories, U.S. Environmental Protection Agency, Office of Water, Washington, DC, EPA822R04005, 2006, http://epa.gov/waterscience/criteria/drinking/March 07, 2006.
[7] J. Valenzuela, U. Bumann, R. Cespedes, L. Padilla, B. Gonzalez, Appl. Environ. Microbiol. 63 (1997) 227.
[8] Z. Aksu, J. Yener, Waste Manage. 21 (2001) 695.
[9] S.S. Gupta, M. Stadler, C.A. Noser, A. Ghosh, B. Steinhoff, D. Lenoir, C.P. Horwitz, K.W. Schramm, T.J. Collins, Science 296 (2002) 326.
[10] G.A. Henke, Bioremediation, in: Ullmann's Encyclopedia of Industrial Chemistry, Wiley-VCH Verlag GmbH, Weinheim, Germany, 2002 (Electronic Release).
[11] M. Pera-Titus, V. Garcya-Molina, M.A. Banos, J. Gimenez, S. Esplugas, Appl. Catal. B 47 (2003) 219.
[12] R. Oliveira, M.F. Almeida, L. Santos, M. Madeira, Ind. Eng. Chem. Res. 45 (2006) 1266.
[13] W.E. Pereira, C.E. Rostad, C.T. Chiou, T.I. Brinton, L.B. Barber, D.K. Demchech, C.R. Demas, Environ. Sci. Technol. 22 (1988) 772.
[14] W. Chu, C.Y. Kwan, K.H. Chan, S.K. Kam, J. Hazard. Mater. B121 (2005) 119.
[15] R.-A. Doong, R.A. Maithreepala, S.-M. Chang, Water Sci. Technol. 42 (2002) 253.
[16] L. Norena-Franco, I. Hernandez-Perez, J. Aguilar-Pliego, A. Maubert-Franco, Catal. Today 75 (2002) 189.
[17] Q. Wu, X. Hu, P.L. Yue, X.S. Zhaob, G.Q. Lub, Appl. Catal. B: Environ. 32 (2001) 151.
[18] N. Srinivas, V. Radha Rani, S.J. Kulkarni, K.V. Raghavan, J. Mol. Catal. A: Chem. 179 (2002) 221.
[19] J.S. Beck, J.C. Vartuli, W.J. Roth, M.E. Leonowicz, C.T. Kresge, K.D. Schmitt, C.T.-W. Chu, D.H. Olsen, E.W. Sheppard, S.B. Mc Cullen, J.B. Higgins, J.L. Schlenker, J. Am. Chem. Soc. 114 (1992) 10834.
[20] F. Bergaya, M. Vayer, Appl. Clay Sci. 12 (1997) 275.

[21] C.H. Rhee, J.S. Lee, Catal. Today 38 (1997) 213.
[22] S. Schwarz, D.R. Corbin, A.J. Vega, in: R.F. Lobo, J.S. Beck, S.L. Suib, D.R. Corbin, M.E. Davis, L.E. Iton, S.I. Zones (Eds.), Materials Research Society Symposium Proceedings, vol. 431, Materials Research Society, Pittsburg, PA, 1996, p. 137.
[23] A. Liepold, K. Ross, W. Reschetilowski, A.P. Enculcas, J. Rocha, A. Philippou, M.W. Anderson, J. Chem. Soc., Faraday Trans. 92 (1996) 4623.
[24] C.A. Koh, R. Nooney, S. Tahir, Catal. Lett. 47 (1997) 199.
[25] M.G.F. Rodrigues, Ceramica 49 (2003) 146.
[26] G.C. Bond, Heterogeneous Catalysis, Oxford Science Publications, Clarendon Press, Oxford, 1987, pp. 28–30.
[27] M. Stoyanova, St. Christoskova, M. Georgieva, Appl. Catal. A: Gen. 249 (2003) 295.